HHS Public Access

Author manuscript

Small. Author manuscript; available in PMC 2016 October 01.

Published in final edited form as:

Small. 2015 October ; 11(38): 5079–5087. doi:10.1002/smll.201500906.

Differences in the Toxicological Potential of Two-Dimensional versus Aggregated Molybdenum Disulfide in the Lung

Xiang Wang[†,‡], **Nikhita D. Mansukhani**[ς], **Linda M. Guiney**[ς], **Zhaoxia Ji**[‡], **Chong Hyun Chang**[‡], **Meiying Wang**[†], **Yu-Pei Liao**[†], **Tze-Bin Song**[&], **Bingbing Sun**[†], **Ruibin Li**[†], **Tian Xia**[†,‡], **Mark C. Hersam**[ς], and **André E. Nel**[†,‡,*]

[†]Division of NanoMedicine, Department of Medicine; University of California, Los Angeles, CA 90095, United States

[‡]California NanoSystems Institute; University of California, Los Angeles, CA 90095, United States

[ς]Departments of Materials Science and Engineering, Chemistry, and Medicine, Northwestern University, Evanston, Illinois 60208, United States

[&]Department of Materials Science and Engineering, University of California, Los Angeles, CA 90095, United States

Abstract

Two-dimensional molybdenum disulfide (MoS_2) has distinct optical and electronic properties compared to aggregated MoS_2, enabling wide use of these materials for electronic and biomedical applications. However, the hazard potential of MoS_2 has not been studied extensively. Here, we present a comprehensive analysis of the pulmonary hazard potential of three aqueous suspended forms of MoS_2: aggregated MoS_2 (Agg-MoS_2), MoS_2 exfoliated by lithiation (Lit-MoS_2) and MoS_2 dispersed by Pluronic F87 (PF87-MoS_2). No cytotoxicity was detected in THP-1 and BEAS-2B cell lines. However, Agg-MoS_2 induced strong pro-inflammatory and pro-fibrogenic responses *in vitro*. In contrast, Lit- and PF87-MoS_2 had little or no effect. In an acute toxicity study in mice, Agg-MoS_2 induced acute lung inflammation, while Lit-MoS_2 and PF87-MoS_2 had little or no effect. In a sub-chronic study, there was no evidence of pulmonary fibrosis in response to all forms of MoS_2. These data suggest that exfoliation attenuates the toxicity of Agg-MoS_2, which is an important consideration towards the safety evaluation and use of nanoscale MoS_2 materials for industrial and biological applications.

Keywords

Molybdenum Disulfide; Cytotoxicity; Pulmonary Toxicity; Hazard Assessment

[*]Corresponding Author: André E. Nel, Department of Medicine, Division of NanoMedicine, UCLA School of Medicine, 52-175 CHS, 10833 Le Conte Ave, Los Angeles, CA 90095-1680. Tel: (310) 825-6620, Fax: (310) 206-8107, anel@mednet.ucla.edu.

Supporting Information

Supporting Information is available from the Wiley Online Library.

1. Introduction

Molybdenum disulfide (MoS_2), a typical transition metal dichalcogenide, is a flat tri-layer material composed of a layer of molybdenum bonded on either side to layers of sulfur.[1] It has generated significant attention as a post-graphene two-dimensional material due to its extraordinary electronic, optical, and physical properties that lend themselves to a wide variety of applications including catalysis, electronics, and therapeutics.[1, 2] Among different production methods of nanoscale two-dimensional MoS_2 (2D-MoS_2), solution-based processing promises exceptional scalability and low cost, and thus represents the most probable path for incidental exposure including pulmonary exposure.[3, 4] As solution-based nanoscale MoS_2 is poised to enter the market, it is essential to identify its toxic potential and develop safe methods for handling nanoscale MoS_2.

MoS_2 is currently used in spray and automobile lubrication products in the market place in its bulk form, with the potential to lead to aerosolized inhalation exposure in humans. In fact, most reports on MoS_2 are for the bulk form, which demonstrated good *in vivo* biocompatibility by the U.S. Public Health Service.[5] No fatalities or adverse health effects were observed in rats and guinea pigs following inhalation exposure to the bulk materials.[5] The low toxicity is attributed to MoS_2 being chemically inert and insoluble in body fluids. However, no comprehensive hazard assessment work has been conducted for nanoscale MoS_2 materials to date. In order to assess the potential toxicity of solution-based nanoscale MoS_2 materials, we established a representative test library that includes three aqueous forms of nanoscale MoS_2: aggregated MoS_2 (Agg-MoS_2) and two dispersed types of nanoscale MoS_2: one that is chemically exfoliated by lithium ion intercalation (Lit-MoS_2), and another that is dispersed using ultrasonication in the presence of a biocompatible block copolymer, Pluronic F87 (PF87-MoS_2). These three samples are representative of the possible aqueous nanoscale dispersions of MoS_2 that may enter the market for the aforementioned applications, spanning chemically and ultrasonically exfoliated, as well as non-surfactant and surfactant stabilization, respectively.

Against this background, we set out to determine whether nanoscale MoS_2 materials pose a biological hazard *in vitro* and *in vivo*. We demonstrate that while Agg-MoS_2 is capable of inducing strong pro-inflammatory and pro-fibrogenic responses *in vitro*, Lit- and PF87-MoS_2 had little or no effects. In an acute oropharyngeal exposure study in mice, Agg-MoS_2 induced acute lung inflammation, while Lit- and PF87-MoS_2 had decreased inflammation or no effects. In a sub-chronic study, all forms of MoS_2 did not induce lung fibrosis. Our data suggest that the exfoliation process attenuates the hazard potential of nanoscale 2D-MoS_2 compared to Agg-MoS_2. Overall, these results suggest strategies for the safe use of nanoscale 2D-MoS_2 materials in industrial and biomedical applications.

2. Results and Discussion

2.1. Preparation and Characterization of Molybdenum Disulfide (MoS_2)

All MoS_2 samples were prepared from an original batch of the bulk material. Pluronic F87 dispersed MoS_2 (PF87-MoS_2) was prepared by ultrasonication of MoS_2 powder in a solution of PF87 in DI water. Pluronic® is a non-ionic triblock copolymer composed of two

hydrophilic poly (ethylene oxide) (PEO) end pieces and a central hydrophobic poly (propylene oxide) (PPO) segment.[6] Previous studies have demonstrated that several types of Pluronic can effectively disperse carbon nanotubes (CNTs) and graphene due to the amphiphilic nature of these polymers, providing electrosteric hindrance of the coated surface.[7-9] Because Pluronic colloid interactions are subject to the particle dimensions and the length of the polymer chains, PF87 was chosen for its enhanced ability to disperse MoS_2 at high concentrations.[10] Aggregated MoS_2 was prepared by flocculation of PF87-MoS_2. Since lithium intercalation is the most widely used method for chemical exfoliation of bulk MoS_2 into 2D-MoS_2, lithiated MoS_2 (Lit-MoS_2) was synthesized by exposing the bulk powder to a n-butyllithium solution, followed by bath sonication, purification and concentration procedures.[11]

Agg-, Lit- and PF87-MoS_2 were comprehensively characterized. While Agg-MoS_2 is beyond the size range for AFM measurements, scanning electron microscopy (SEM) analysis shows that these particles span several microns in width and thickness (Figure 1A). AFM assessment of PF87-MoS_2 show that these particles have a mean square root surface area of 27.6 ± 15.6 nm and an average height of 5.2 ± 1.1 nm (Figure 1B, E and F). Similar measurements show that the Lit-MoS_2 particles are larger than PF87-MoS_2, which have a mean square root surface area of 187.5 ± 126.9 nm and a mean height of 3.9 ± 0.6 nm (Figure 1C, E and F). The hydrodynamic sizes of Agg- and Lit-MoS_2 suspended in RPMI 1640 are smaller than BEGM due to the presence of fetal bovine serum (FBS). PF87-MoS_2 is better dispersed than Agg- and Lit-MoS_2 in both media (Table 1). The zeta potentials of the three material types were in the range of −4.3 to −8.8 mV in cell culture media, and −12.9 to −34.3 mV in water (Table 1).

2.2. 2D-MoS_2 exerts less pro-inflammatory effects than Agg-MoS_2 *in vitro*

We determined the pro-inflammatory responses of MoS_2 using THP-1 and BEAS-2B cell lines. The myeloid cell line, THP-1, was chosen because it can be differentiated into a lineage with macrophage-like properties,[12] while BEAS-2B cells are derived from human bronchial epithelial cells.[13] These cell types are representative of the cell types that provide the first line of defense at the portal of entry into the lung. Use of these cells demonstrated in an MTS assay that none of the MoS_2 form variations had an effect on cell viability (Figure 2A, B). It is noteworthy that literature show that some types of nanomaterials, including MoS_2, have interference with MTT reagent at high dose level (> 100 μg/mL) when measuring the absorbance at 490 nm.[14-17] Accordingly, we conducted an abiotic experiment to measure the absorbance of the mixture of MoS_2 and MTS reagent at 490 nm. We found that there was no interferences between MoS_2 and MTS reagent within the dose range (0 to 50 μg/mL) we in this work (data not shown). Additionally, the MTS results were confirmed in a different viability assay, i.e. a luminescence-based cellular assay that determines ATP content as a measure of viability (Figure S1A, B). When testing pro-inflammatory cellular effects, however, we observed that while Agg-MoS_2 induced significant increases in IL-8, TNF-α and IL-1β production, there were significantly less effects of Lit- or PF87-MoS_2 on cytokine and chemokine production in BEAS-2B and THP-1 cells (Figure 3B and C). These cytokines and chemokines play important roles in lung inflammation in response to inhaled foreign materials. IL-8, known as a neutrophil

chemotactic factor, can induce neutrophil chemotaxis and migration toward sites of particle deposition and inflammation.[18, 19] TNF-α is a member of a group of macrophage-derived cytokines that also play a role in acute inflammation.[20] IL-1β is an important mediator of acute and sub-chronic inflammatory responses, which can also lead to fibrogenic effects in response to particulate substances and fibers in the lung.[12, 21] Agg-MoS_2 also induced increased TGF-β1 and PDGF-AA production in a co-culture of THP-1 with BEAS-2B cells (Figure S1C and D). These growth factors could be significant from the perspective of pro-fibrogenic pulmonary responses since synergy with IL-1β during epithelial-mesenchymal transition in the lung in response to carbon nanotubes, graphene and asbestos fibers plays a key role in pulmonary fibrosis.[21-23] Whether growth factor production will result in pulmonary fibrosis is dependent on the magnitude and duration of the pulmonary response, which is shaped by the dose, lung burden, removal and persistence of the material.[21, 23, 24]

Bioavailability plays an important role in engineered nanomaterials (ENM)-induced cellular responsiveness.[25-28] Under experimental conditions, the colloidal stability of the aqueous suspended materials can affect the sedimentation and contact of the materials with cells on the surface of the tissue culture dish.[29] Assessment of the suspension stability index of the various MoS_2 materials in BEGM and RPMI 1640 demonstrated that, while PF87-MoS_2 showed excellent stability in both culture media, Agg-MoS_2 was the least stable (Figure S2A and B), leading to rapid settling at the bottom of the dishes. Since this could lead to enhanced bioavailability, confocal Raman spectroscopy was used to assess MoS_2 uptake in THP-1 cells; MoS_2 yields characteristic peaks at 382 and 406 nm (Figure S3). While Agg-MoS_2 was associated with a robust Raman signature, less pronounced peaks were observed for Lit- and PF87-MoS_2 (Figure S3). Since the Raman signal is not quantitative, we also used ICP-OES to assess cellular content. This measurement demonstrated that Agg-MoS_2 was present in higher abundance, compared to other materials (Figure 1C and D), with PF87-MoS_2 showing the least cellular association. Since these data show good correlation to the lesser pro-inflammatory effects of PF87-MoS_2, it would appear that bioavailability of the materials could indeed determine the effects on cytokine and chemokine production.

2.3. 2D-MoS_2 exerted less acute pro-inflammatory effects in the lung than Agg-MoS_2

MoS_2 materials are currently used in spray and automobile lubrication products in the market place, with the potential to lead to aerosolized exposure upon inhalation in humans. To determine if MoS_2 poses pulmonary hazard potential, we used oropharyngeal aspiration to compare our characterized MoS_2 materials in C57Bl/6 mice. Due to the absence of MoS_2 exposure data in humans, we used, for comparison, exposure data for MWCNTs in a production laboratory, where the airborne concentration of the tubes can be as high as 400 $\mu g/m^3$. [30] Assuming a ventilation rate of 20 L/min in healthy human subjects [31] and a particle deposition fraction of 30 %, the estimated exposure (8 h/day, 5 d/week for 16 weeks) of an adult could reach 92.16 mg. Using a human lung alveolar surface area of 102 m^2,[32] this is equivalent to a deposition level of 903.53 $\mu g/m^2$ in the lung (Table S1). This equals a dose of 1.81 mg/kg in a 25 g mouse with an alveolar epithelial surface area of 0.05 m^2.[32] Accordingly, we decided on a 2 mg/kg dose for bolus instillation studies in mice. The positive control included oropharyngeal delivery of 5 mg/kg of Min-U-Sil (α-quartz), a highly inflammogenic material associated with both acute and sub-chronic lung toxicity.

Forty hours after oropharyngeal aspiration, Min-U-Sil could be seen to induce significant increases in LIX (LPS-induced CXC chemokine), MCP-1 (monocyte chemoattractant protein-1), IL-6 levels and neutrophil counts in the bronchoalveolar lavage fluid (BALF), along with mild inflammatory changes in the lung (Figure 4 A-E). While Agg-MoS_2 induced robust LIX (Figure 4A), MCP-1 (Figure 4B), and IL-6 responses (Figure 4C) along with neutrophilic exudation into the BALF (Figure 4D), Lit- and PF87-MoS_2 did not trigger cytokine or chemokine production in the lung (Figure 4A, B and C). Moreover, the exfoliated materials only mounted mild neutrophilic increases in the BALF (Figure 4D). Histopathological changes in animal lungs confirmed these differential effects (Figure 4E), with Agg-MoS_2 inducing focal areas of inflammation around small airways, while Lit- and PF87-MoS_2 had little or no effect (Figure 4E).

It is helpful for predictive toxicological modeling to be able to reconcile *in vitro* with *in vivo* dosimetry. We used the lung alveolar epithelium surface area to calculate a surface area dose (SAD) in the mouse. An animal exposed to 2 mg/kg MoS_2 is equivalent to a SAD of 1 mg/m^2 in a 25 g mouse with an alveolar epithelium surface area of 0.05 m^2.[32] Assuming that the MoS_2 dose is homogeneously distributed in the tissue culture dish and that the thickness of a cell layer is ~ 15 μm, the *in vitro* exposure dose would be ~ 66 μg/mL. Thus, the *in vitro* dose range (6.25 - 50 μg/mL) that we chose is comparable to the dose in the mouse experiment.

2.4. 2D- as well as Agg-MoS_2 failed to induce sub-chronic inflammatory effects in the lungs of mice

We also determined the sub-chronic effects of MoS_2 in the lung, 21 days post-exposure. Examination of the BALF showed that neutrophil influx had largely disappeared at this point for all of the MoS_2 materials, while quartz still resulted in residual inflammation (not shown). Moreover, Min-U-Sil aspiration was associated with increased levels of TGF-β1 (Figure 5A) and PDGF-AA (Figure 5B) in the BALF, confirming its pro-fibrogenic potential. However, while Agg-MoS_2 and Lit-MoS_2 induced significant increases of the TGF-β1 in the BALF, none of the MoS_2 materials had an effect on PDGF-AA production (Figure 5A and B). While Min-U-Sil resulted in increased collagen production at 21 days, as determined by a Sircol assay (Figure 5C) as well as Masson's trichrome staining (Figure 5D), none of the MoS_2 materials resulted in increased collagen production or interstitial collagen deposition in the lungs of exposed animals (Figure 5D).

All considered, there is good agreement between the *in vivo* and *in vitro* hazard ranking of MoS_2 in spite of differences in the cellular handling in the lung versus tissue culture conditions. While sedimentation of Agg-MoS_2 is likely a major determinant for cellular uptake and bioavailability in the tissue culture dish (Figure 2C and D), its uptake by epithelial cells and macrophages in the lung takes place at deposition sites where the aqueous carrier is absorbed or removed by the ciliary escalator. Thus, the role of sedimentation at deposition sites in the lung is likely to be limited, with the state of dispersion determining how widespread the dissemination of the particles will be. It is interesting, therefore, that ICP-OES analysis demonstrated less variation in the lung content of the various MoS_2 materials 40 h after initial aspiration (Figure 6A). While slightly less

for Lit-MoS_2 and PF87-MoS_2 than Agg-MoS_2, the lung content was not statistically significant among the materials and therefore quite different from the variation seen in the cellular studies (Figure 2C and D). This was confirmed by Raman confocal microscopy, which showed prominent MoS_2 peaks for all MoS_2 materials in alveolar macrophages (Figure S4A). Thus, the lung burden and acute *in vivo* bioavailability do not explain the failure of the exfoliated materials to induce acute lung inflammation. A similar trend was seen for ICP-OES analysis at 21 d, at which point the lung burden was considerably reduced (Figure 6B). While there was less retention of PF87-MoS_2, the lung contents of Agg- and PF87-MoS_2 were similar. This suggests that the absent or reduced inflammatory effects of the exfoliated materials in the lung has less to do with the total dose than the decreased inflammogenic potential of Lit- and PF87-MoS_2 in the lung. This could be a function of the surface reactivity of the materials and/or their state of dispersal. In addition to improving material dispersal, Pluronic coating of MWCNTs, SWCNTs, and graphene has been shown to reduce surface reactivity at the cellular or pulmonary interface through steric hindrance.[7-9] Steric hindrance results from binding of the hydrophobic midblock region of the polymer to the hydrophobic surface of these materials, leaving the hydrophilic PEO end-blocks to stand away from the surface, thereby providing a protective coating.[9] We propose that PF87 plays a similar role on the surface of MoS_2, which prevents the surface from triggering pro-inflammatory cellular responses. Lithiation could also reduce surface reactivity, bioavailability or may act to increase the clearance of MoS_2 in the lung. Altogether, these data show that 2D-MoS_2 nanomaterials are safer than Agg-MoS_2.

Data about the safety of 2D-MoS_2 materials are limited. Recently, Pumera *et al.* reported that under *in vitro* conditions, MoS_2 nanosheets failed to affect the viability of A549 cells when compared to other transition-metal dichalcogenides (TMDs), including WSe_2.[16] However, the same group also demonstrated that MoS_2 nanosheets, obtained through the use of n-butyllithium (n-Bu-Li) or tert-butyllithium (t-Bu-Li) as exfoliating agents, can be cytotoxic at high dose range (200 to 400 μg/mL).[16, 17] While it is difficult to interpret this data without more comprehensive information about the physicochemical characterization of these materials, it is possible that material aggregation at high dose or the presence of residual lithium ions could be involved in the toxicity outcome. Moreover, the use of cytotoxicity as the sole criterion of material hazard may not reveal sublethal effects, such as the pro-inflammatory responses in cells and the lung, as we show in this study. Also the high dose levels used by Pumera *et al.* may not be representative of real life exposure conditions. We believe our study provides more realistic exposure conditions, ultimately leading to the conclusion that 2D-MoS_2 nanomaterials are relatively safe.

3. Conclusion

In summary, we addressed the lack of hazard assessment for nanoscale MoS_2 by performing comprehensive *in vitro* and *in vivo* toxicological analysis for exfoliated vs. aggregated MoS_2 materials. Our results demonstrate that 2D-MoS_2, including Lit- and PF87-MoS_2, elicit significantly reduced pro-inflammatory effects compared to Agg-MoS_2 at cellular and lung levels. In addition, all MoS_2 formulations did not induce sub-chronic effects in the lung. The reduced hazard of 2D-MoS_2 materials is correlated to improved dispersion and surface coating, which play important roles in determining the bioavailability and surface reactivity

of the exfoliated materials. These data suggest that 2D-MoS_2 materials are safer than Agg-MoS_2, which may promote the safe use of 2D-MoS_2 for industrial and biomedical applications.

4. Experimental Section

4.1. Preparation of Nanoparticle suspensions

The molybdenum disulfide (MoS_2) dispersions were prepared as follows: For lithiated MoS_2 (Lit-MoS_2), lithium ion intercalation was achieved by exposing 300 mg of MoS_2 powder (Sigma Aldrich) to 3 mL of 1.6 M butyllithium solution in hexane while gently stirring for 48 h in an Argon-filled glovebox. The slurry was subsequently transferred to a filter and rinsed with 60 mL hexane. Upon removal from the glovebox, the powder was immersed in 500 mL DI water and bath sonicated immediately to prevent de-intercalation and promote full exfoliation of the MoS_2. The exfoliated solution was briefly centrifuged to remove non-exfoliated MoS_2 and then dialyzed for 7 days to remove excess lithium and hexane. Finally, the solution was removed from dialysis and concentrated using vacuum filtration. Pluronic F87 dispersed MoS_2 (PF87-MoS_2) was prepared by immersing 300 mg of MoS_2 powder in 8 mL 2 % w/v PF87 (BASF) solution in DI water, and then ultrasonicated for 1 h at an amplitude of approximately 16 Watts. The slurry was centrifuged to remove any non-exfoliated material and aggregates by retaining only the top 80 % of the supernatant. The solution was dialyzed for three days and concentrated using vacuum evaporation. The aggregated MoS_2 (Agg-MoS_2) was prepared from the PF87 dispersion by inducing flocculation through the addition of four parts isopropyl alcohol to one part PF87-MoS_2. The aggregates were filtered from the solution and rinsed thoroughly with DI water, and then resuspended by bath sonication in DI water. The concentrations of the MoS_2 solutions were measured using ICP-MS as described previously.[33] Briefly, MoS_2 solutions were digested overnight at 65 °C in nitric acid and subsequently diluted with water and internal standard. Using the ICP-MS measurements, concentration was inferred stoichiometrically.

4.2. Cell culture and co-incubation with Molybdenum Disulfide

BEAS-2B and THP-1 cells were obtained from ATCC (Manassas, VA). 1×10^4 BEAS-2B cells were cultured in 0.1 mL BEGM in 96-well plates at 37 °C. THP-1 cells were pretreated with 1 μg/mL phorbol 12-myristate acetate (PMA) overnight and primed with 10 ng/mL lipopolysaccharide (LPS) to provide transcriptional activation of the IL-1β precursor.[12] Both types of cells were subsequently cultured in 96-well plates (Costar, Corning, NY, USA) at 37 °C for 24 h. MoS_2 suspensions were added to these cultures at 6.25- 50 μg/mL. After 24 h of culture, the supernatants were collected for the measurement of IL-8, TNF-α, and IL-1β levels (BD Biosciences, San Diego, CA), using ELISA kits. Cytokine levels were expressed as pg/mL.

4.3. Cytotoxicity Assessment

Cytotoxicity was determined by an MTS assay, which was carried out with CellTiter 96 Aqueous (Promega Corp.) kit. 1×10^4 BEAS-2B or 3×10^4 THP-1 cells in 100 μL of culture medium were plated in each well of a 96 multiwell plate (Costar, Corning, NY) for overnight growth. The medium was removed, and cells were treated for 24 h with 100 μL of

6.25-50 μg/mL MoS_2 suspensions. After the treatment, the cell culture medium was removed and followed by washing of the plates three times with PBS. Each well received 120 μL of culture medium containing 16.7 % of MTS stock solution for 1 h at 37 °C in a humidified 5 % CO_2 incubator. The plate was centrifuged at 2000 g for 10 min in NI Eppendorf 5430 with a microplate rotor to spin down the cell debris. An 85 μL amount of the supernatant was removed from each well and transferred into a new 96 multiwell plate. The absorbance of formazan was read at 490 nm on a SpectraMax M5 microplate reader (Molecular Devices Corp., Sunnyvale, CA, USA).

4.4. Oropharyngeal aspiration studies in mice

Eight-week-old male C57Bl/6 mice received oropharyngeal aspiration of Agg-MoS_2, Lit- or PF87-MoS_2 materials, as previously described.[12] Briefly, 2 mg/kg of each type of MoS_2 suspension was instilled at the back of the tongue in 50 μL water in anesthetized animals. Control animals received the same volume of water. Crystalline silica (Min-U-Sil) was used as a positive control at 5 mg/kg. The mice were sacrificed after 40 h and 21 days, respectively, to assess acute and sub-chronic effects. BALF and lung tissue were collected for measurement of LIX, MCP-1, IL-6, TGF-β1, and PDGF-AA levels and performance of Hematoxylin and Eosin (H&E) or Masson's trichrome staining. The detailed methods appear in the Supporting Information.

4.5. Statistical Analysis

Mean and standard deviation (SD) were calculated for each parameter. Results were expressed as mean ± SD of multiple determinations. Comparisons of each group were evaluated by two-sided Student's t tests. A statistically significant difference was assumed when p was <0.05.

Supplementary Material

Refer to Web version on PubMed Central for supplementary material.

Acknowledgements

This work is supported by the US Public Health Service Grant, RO1 ES022698 (NIEHS). Infrastructure support was also provided by the National Science Foundation and the Environmental Protection Agency to UC-CEIN under Cooperative Agreement Number DBI-1266377. Fluorescent microscopy was performed at the CNSI Advanced Light Microscopy/Spectroscopy Shared Facility at UCLA. Any opinions, findings, conclusions or recommendations expressed herein are those of the author(s) and do not necessarily reflect the views of the National Science Foundation or the Environmental Protection Agency. This work has not been subjected to an EPA peer and policy review. The findings and conclusions in this article are those of the authors and do not necessarily represent the views of the National Institute for Occupational Safety and Health.

References

[1]. Wang QH, Kalantar-Zadeh K, Kis A, Coleman JN, Strano MS. Nat Nanotechnol. 2012; 7:699–712. [PubMed: 23132225]

[2]. Jariwala D, Sangwan VK, Lauhon LJ, Marks TJ, Hersam MC. ACS nano. 2014; 8:1102–1120. [PubMed: 24476095]

[3]. Kang J, Seo JWT, Alducin D, Ponce A, Yacaman MJ, Hersam MC. Nat Commun. 2014; 5 doi: 10.1038/ncomms6478.

[4]. Gordon RA, Yang D, Crozier ED, Jiang DT, Frindt RF. Phys Rev B. 2002; 65:125407.

[5]. Fairhall, LT.; Dunn, RC.; Sharpless, NE.; Pritchard, EA. The Toxicity of Molybdenum. U. S. Public Health Service, Public Health Bulletin; 1945. p. 293

[6]. Antaris AL, Seo JWT, Green AA, Hersam MC. ACS nano. 2010; 4:4725–4732. [PubMed: 20669897]

[7]. Duch MCB, G.R. Liang YT, Soberanes S, Urich D, Chiarella SE, Campochiaro LA, Gonzalez A, Chandel NS, Hersam MC, Mutlu GM. Nano Lett. 2011; 11:5201–5207. [PubMed: 22023654]

[8]. Mutlu GM, Budinger GRS, Green AA, Urich D, Soberanes S, Chiarella SE, Alheid GF, McCrimmon DR, Szleifer I, Hersam MC. Nano Lett. 2010; 10:1664–1670. [PubMed: 20377197]

[9]. Wang X, Xia T, Duch MC, Ji ZX, Zhang HY, Li RB, Sun BB, Lin SJ, Meng H, Liao YP, Wang MY, Song TB, Yang Y, Hersam MC, Nel AE. Nano Lett. 2012; 12:3050–3061. [PubMed: 22546002]

[10]. Shvartzman-Cohen R, Nativ-Roth E, Baskaran E, Levi-Kalisman Y, Szleifer I, Yerushalmi-Rozen R. J Am Chem Soc. 2004; 126:14850–14857. [PubMed: 15535711]

[11]. Eda G, Yamaguchi H, Voiry D, Fujita T, Chen MW, Chhowalla M. Nano Lett. 2011; 11:5111–5116. [PubMed: 22035145]

[12]. Wang X, Xia T, Ntim SA, Ji Z, Lin S, Meng H, Chung C, George S, Zhang H, Wang M, Li N, Yang Y, Castranova V, Mitra S, Bonner J, Nel AE. ACS nano. 2011; 5:9772–9787. [PubMed: 22047207]

[13]. Zhang HY, Pokhrel S, Ji ZX, Meng H, Wang X, Lin SJ, Chang CH, Li LJ, Li RB, Sun BB, Wang MY, Liao YP, Liu R, Xia T, Madler L, Nel AE. J Am Chem Soc. 2014; 136:6406–6420. [PubMed: 24673286]

[14]. Rosslein M, Elliott JT, Salit M, Petersen EJ, Hirsch C, Krug HF, Wick P. Chem Res Toxicol. 2015; 28:21–30.

[15]. Worle-Knirsch JM, Pulskamp K, Krug HF. Nano Lett. 2006; 6:1261–1268. [PubMed: 16771591]

[16]. Teo WZ, Chng ELK, Sofer Z, Pumera M. Chem-Eur J. 2014; 20:9627–9632. [PubMed: 24976159]

[17]. Chng ELK, Sofer Z, Pumera M. Nanoscale. 2014; 6:14412–14418. [PubMed: 25341082]

[18]. Kim YM, Reed W, Lenz AG, Jaspers I, Silbajoris R, Nick HS, Samet JM. Am J Physiol-Lung C. 2005; 288:L432–L441.

[19]. Singh S, Shi TM, Duffin R, Albrecht C, van Berlo D, Hoehr D, Fubini B, Martra G, Fenoglio I, Borm PJA, Schins RPF. Toxicol Appl Pharm. 2007; 222:141–151.

[20]. Xia T, Kovochich M, Liong M, Madler L, Gilbert B, Shi HB, Yeh JI, Zink JI, Nel AE. ACS nano. 2008; 2:2121–2134. [PubMed: 19206459]

[21]. Bonner JC. Fibrogenesis & tissue repair. 2010; 3:15. [PubMed: 20738867]

[22]. Li RB, Wang X, Ji ZX, Sun BB, Zhang HY, Chang CH, Lin SJ, Meng H, Liao YP, Wang MY, Li ZX, Hwang AA, Song TB, Xu R, Yang Y, Zink JI, Nel AE, Xia T. ACS nano. 2013; 7:2352–2368. [PubMed: 23414138]

[23]. Wang X, Duch MC, Mansukhani N, Ji Z, Liao YP, Wang MY, Zhang HY, Sun BB, Chang CH, Li RB, Lin SJ, Meng H, Xia T, Hersam MC, Nel AE. ACS nano. 2015

[24]. Palomaki J, Valimaki E, Sund J, Vippola M, Clausen PA, Jensen KA, Savolainen K, Matikainen S, Alenius H. ACS nano. 2011; 5:6861–6870. [PubMed: 21800904]

[25]. Holt BD, Short PA, Rape AD, Wang YL, Islam MF, Dahl KN. ACS nano. 2010; 4:4872–4878. [PubMed: 20669976]

[26]. Jia G, Wang HF, Yan L, Wang X, Pei RJ, Yan T, Zhao YL, Guo XB. Environ Sci Technol. 2005; 39:1378–1383. [PubMed: 15787380]

[27]. Kostarelos K, Lacerda L, Pastorin G, Wu W, Wieckowski S, Luangsivilay J, Godefroy S, Pantarotto D, Briand JP, Muller S, Prato M, Bianco A. Nat Nanotechnol. 2007; 2:108–113. [PubMed: 18654229]

[28]. Nel A, Xia T, Madler L, Li N. Science. 2006; 311:622–627. [PubMed: 16456071]

[29]. Wang X, Xia T, Ntim SA, Ji ZX, George S, Meng H, Zhang H, Castranova V, Mitra S, Nel AE. ACS nano. 2010; 4:7241–7252. [PubMed: 21067152]

[30]. Lee JH, Ahn K, Kim SM, Jeon KS, Lee JS, Yu IJ. J Nanopart Res. 2012; 14

[31]. Galer DM, Leung HW, Sussman RG, Trzos RJ. Regul Toxicol Pharm. 1992; 15:291–306.

[32]. Stone KC, Mercer RR, Gehr P, Stockstill B, Crapo JD. Am J Resp Cell Mol. 1992; 6:235–243.

[33]. Lanphere JD, Luth CJ, Guiney LM, Mansukhani ND, Hersam MC, Walker SL. Environ. Eng. Sci. 2014; 32 DOI: 10.1089/ees.2014.0335.

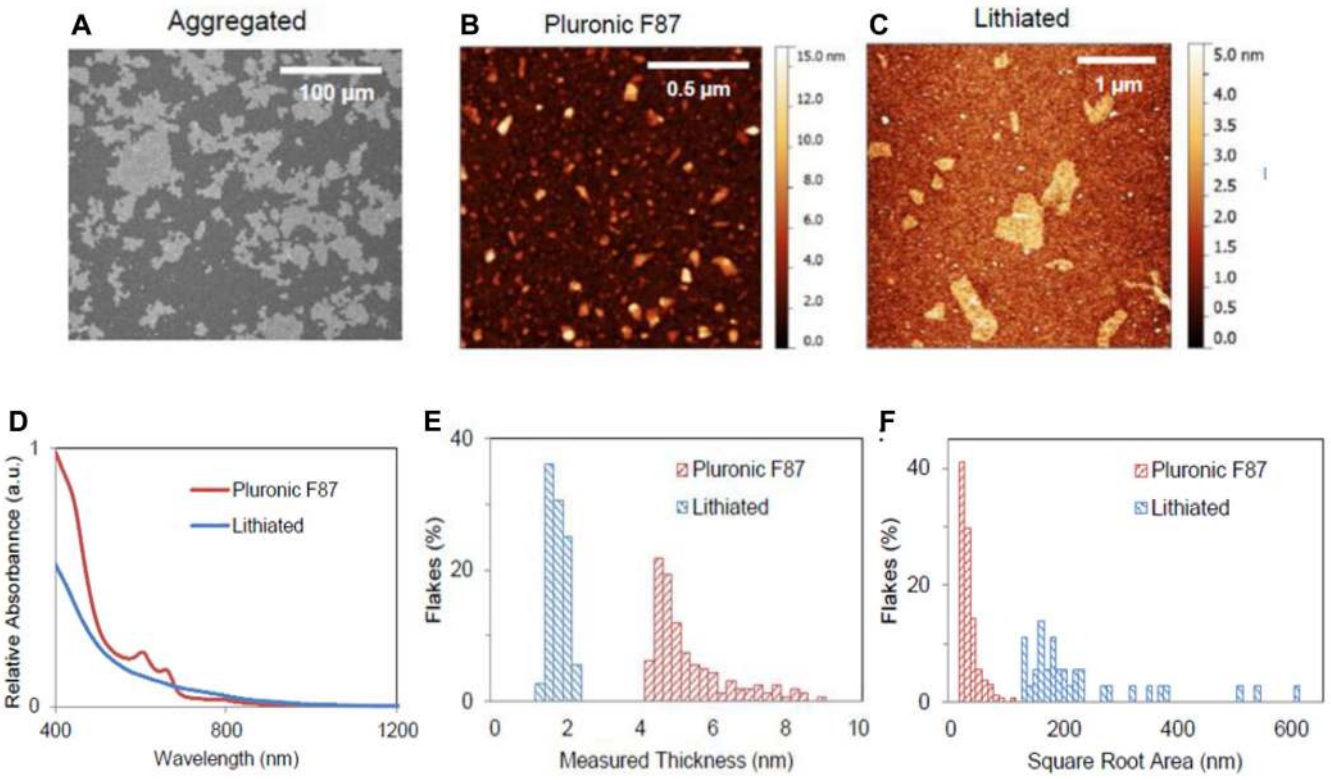

Figure 1.

Characterization of Agg-, Lit- and PF87-MoS_2. (A) Scanning electron micrograph of Agg-MoS_2. (B, C) Representative atomic force microscopy (AFM) images of PF87-MoS_2 and Lit-MoS_2. (D) Optical absorbance spectra of PF87-MoS_2 and Lit-MoS_2. (E, F) AFM histograms of flake thickness and lateral flake sizes in the exfoliated materials.

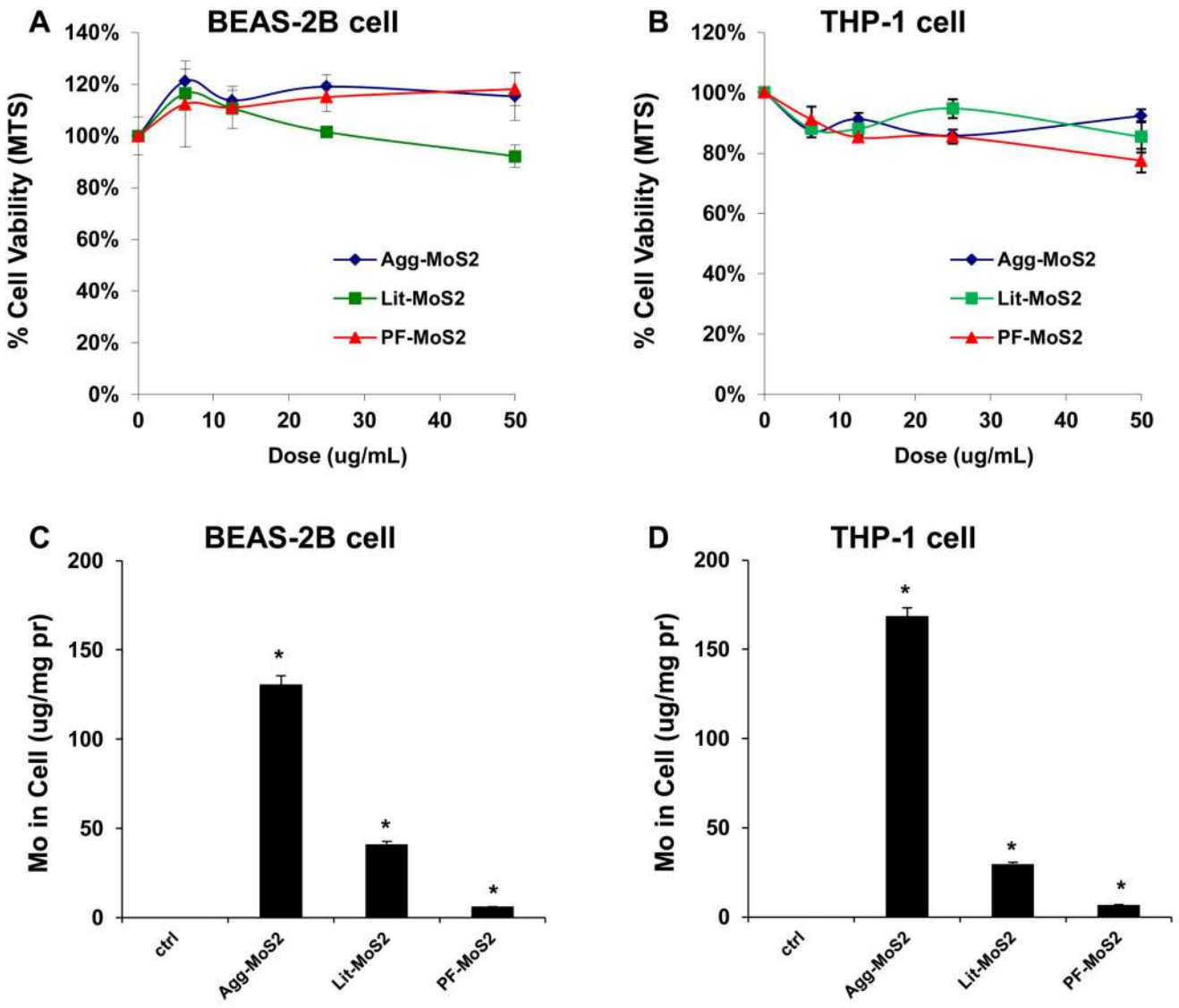

Figure 2.

Cytotoxicity and cellular Mo content in BEAS-2B and THP-1 cells exposed to MoS_2 materials. Assessment of cytotoxicity of MoS_2 on BEAS-2B (A) and THP-1 cells (B). Both cell types were grown in 96-well plates, followed by exposure to 6.25, 12.5, 25 and 50 μg/mL of each of the Agg-, Lit- and PF87-MoS_2 suspensions for 24 h. The media were subsequently washed with PBS and replaced with 120 μL aliquots of the MTS working solution. After incubation for an hour, the plates were centrifuged to collect the supernatants, and their absorbance read at 490 nm in a microplate reader (SpectroMax M5e, Molecular Devices, Sunnyvale, CA). All the MTS values were normalized according to the non-treated control, which was regarded as representing 100 % cell viability. (B) Total cellular Mo content in BEAS-2B (C) and THP-1 (D) cells as determined by ICP-OES. Both cell types were exposed to 50 μg/mL MoS_2 for 24 h, following which the cells were recovered, sonicated and used for acid digestion. The concentration in each sample was expressed as μg Mo per mg of cellular protein.

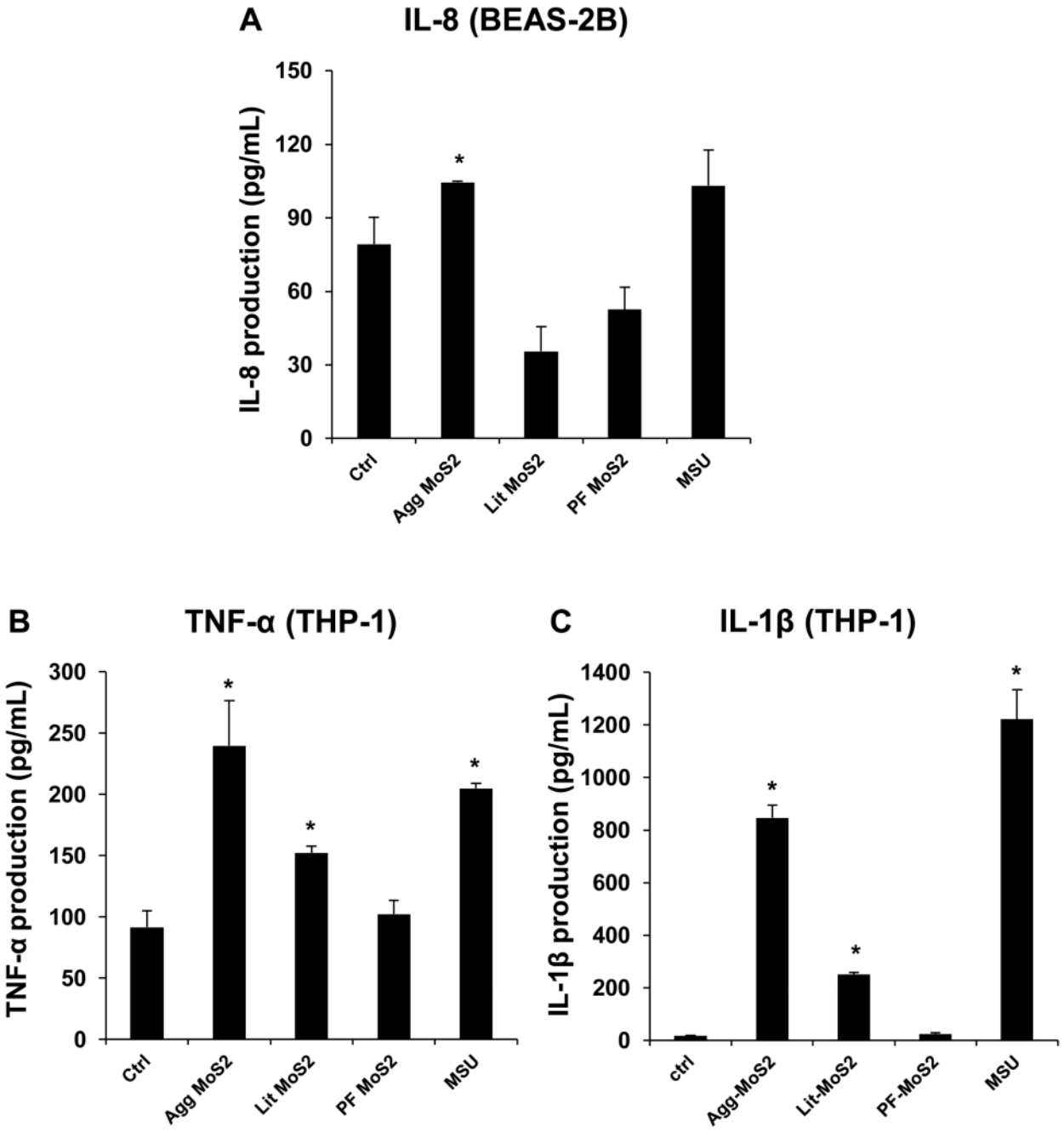

Figure 3.

In vitro pro-inflammatory effects of Agg-, Lit- and PF87-MoS_2. The supernatants from the studies shown in Figure 2 were collected to determine IL-8 (A), TNF-α (B) and IL-1β (C) levels by ELISA. Monosodium urate (MSU) crystals at 100 μg/mL was used as a positive control to measure IL-1β release in response to assembly of the NRLP3 inflammasome. *$p < 0.05$ compared to control.

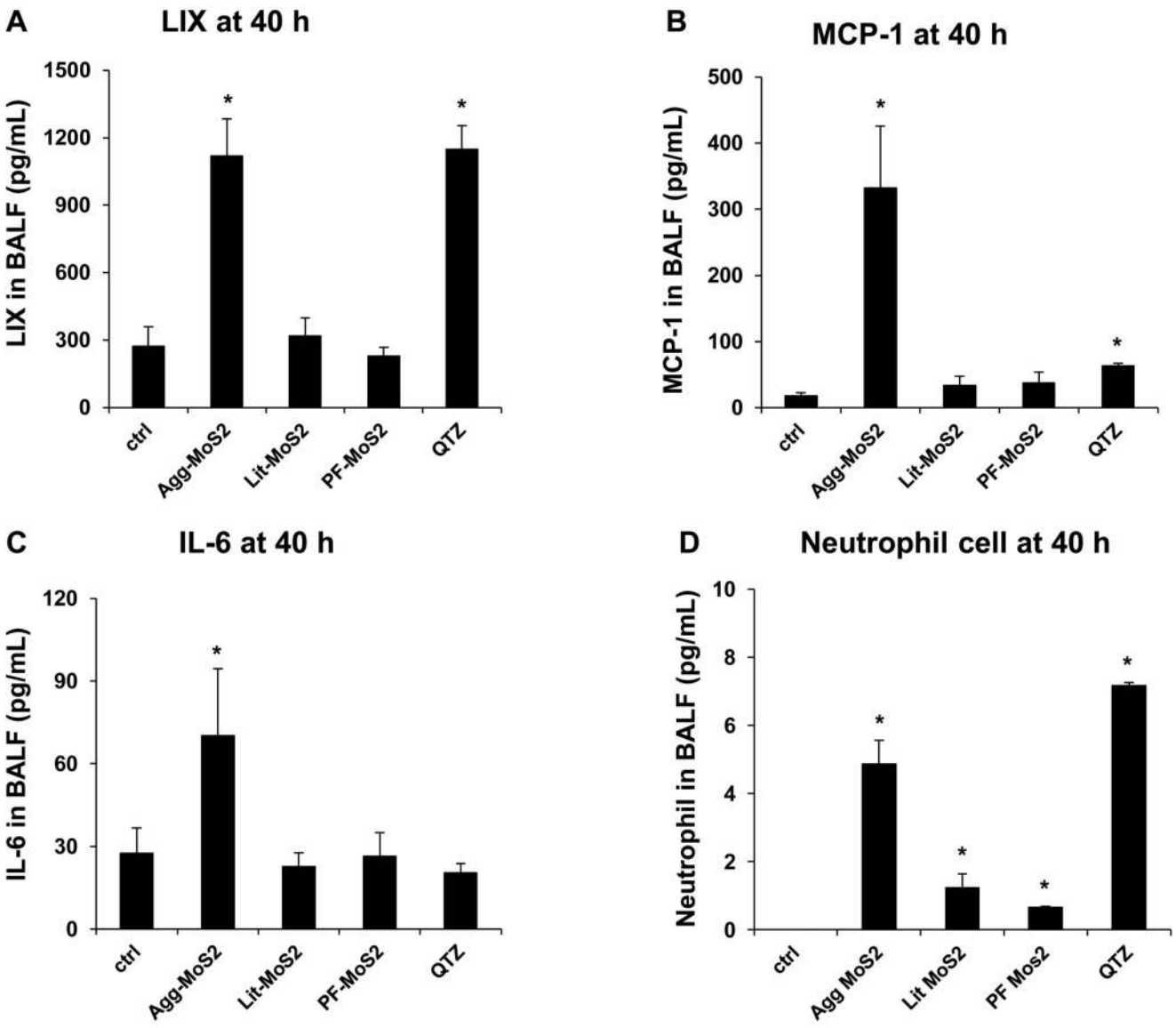

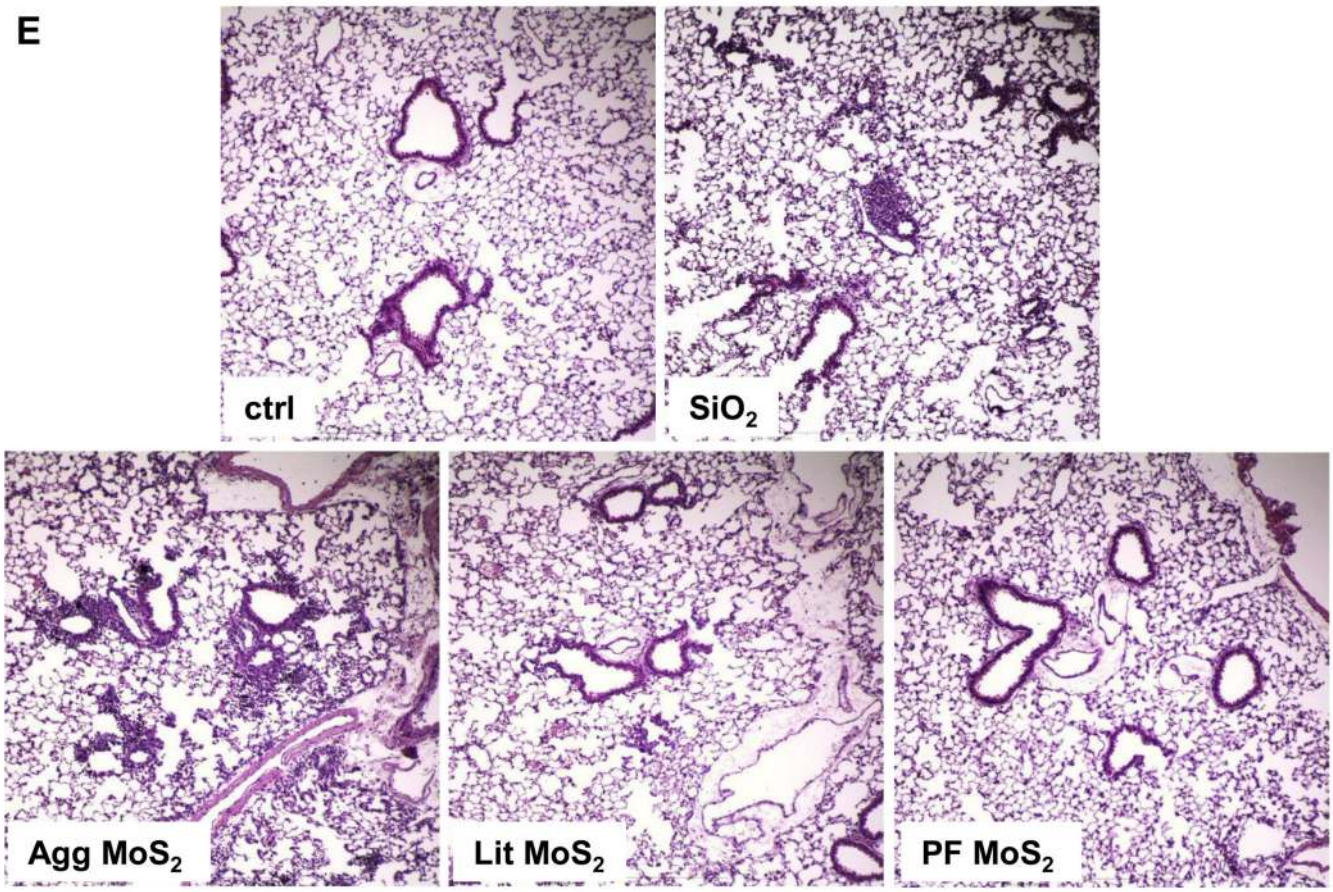

Figure 4.

Acute pulmonary effects of Agg-, Lit- and PF87-MoS_2 in mice. Anesthetized C57BL/6 mice were exposed to dispersed MoS_2 materials, delivered by one-time oropharyngeal aspiration of a bolus dose of 2.0 mg/kg. There were 6 animals per group. Animals were euthanized after 40 h, and BALF was collected to determine LIX (A), MCP-1 (B), and IL-6 (C) levels as well as measuring neutrophil cell counts (D) l. Quartz (QTZ) was used as a positive control, at 5.0 mg/kg. *$p < 0.05$ compared to control. (E) Representative H&E-stained histological images (100 ×) of the lungs of MoS_2 treated mice.

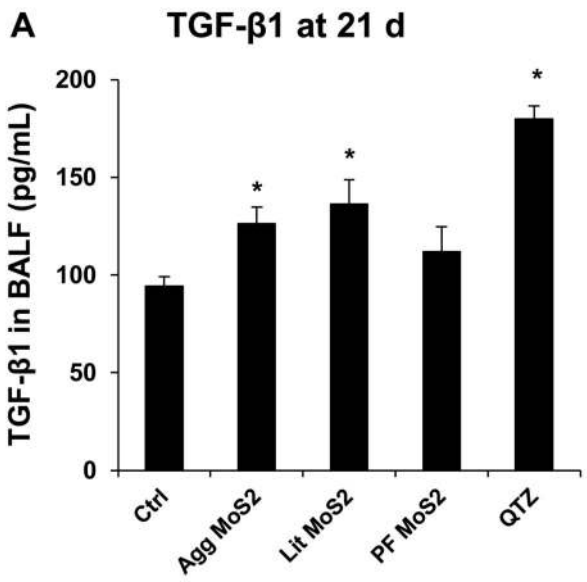

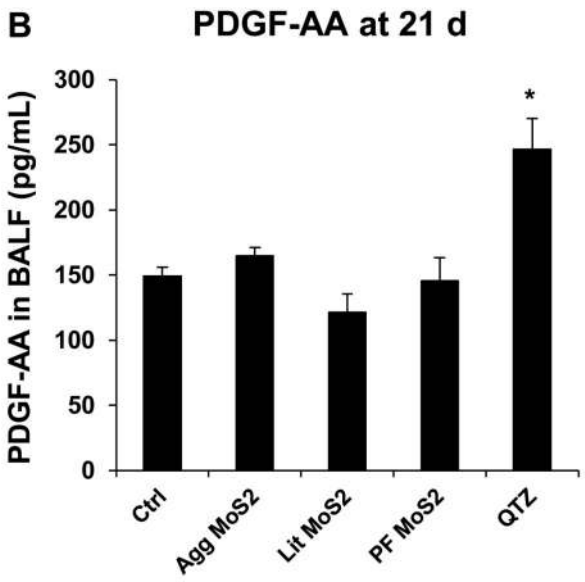

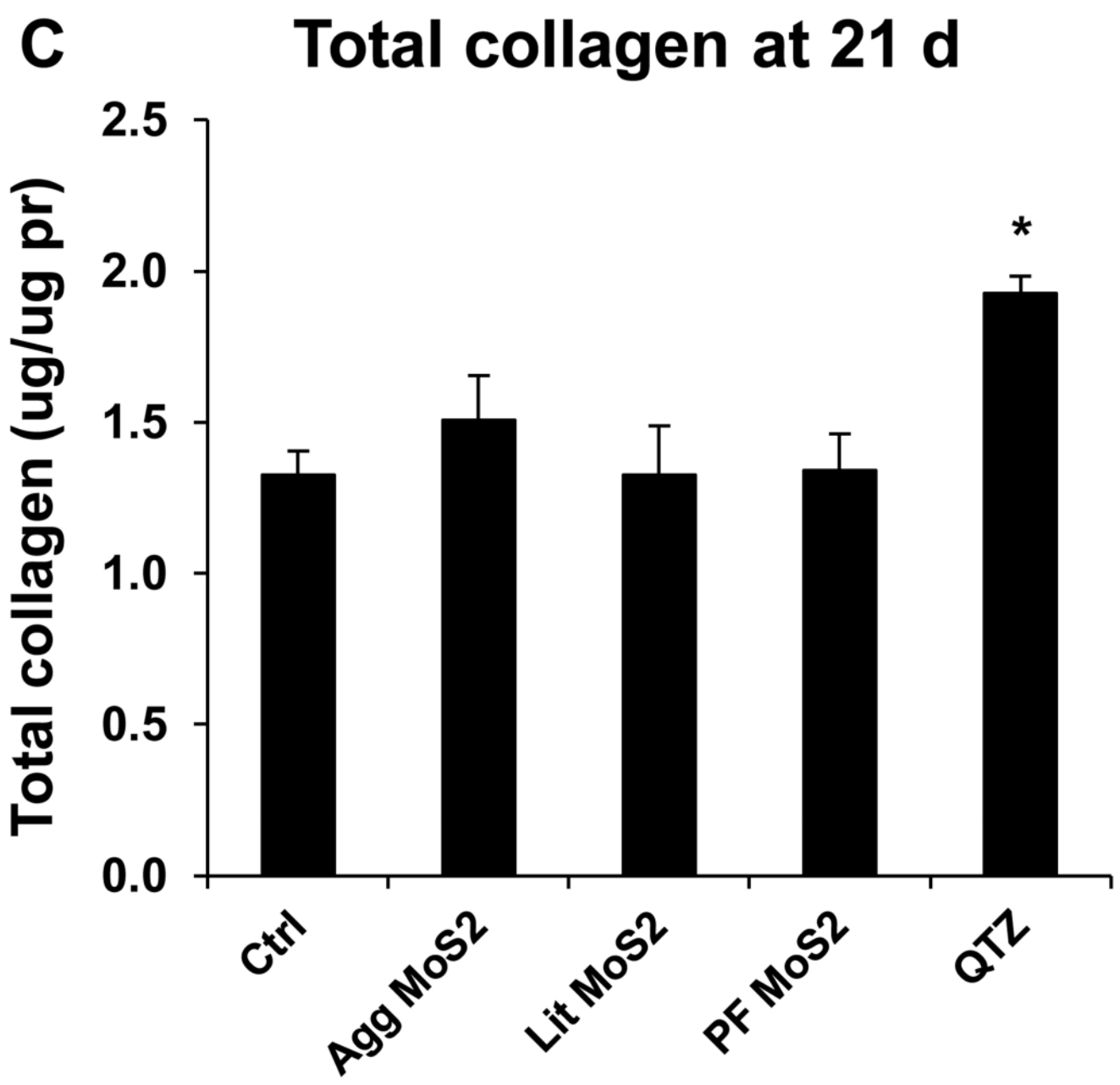

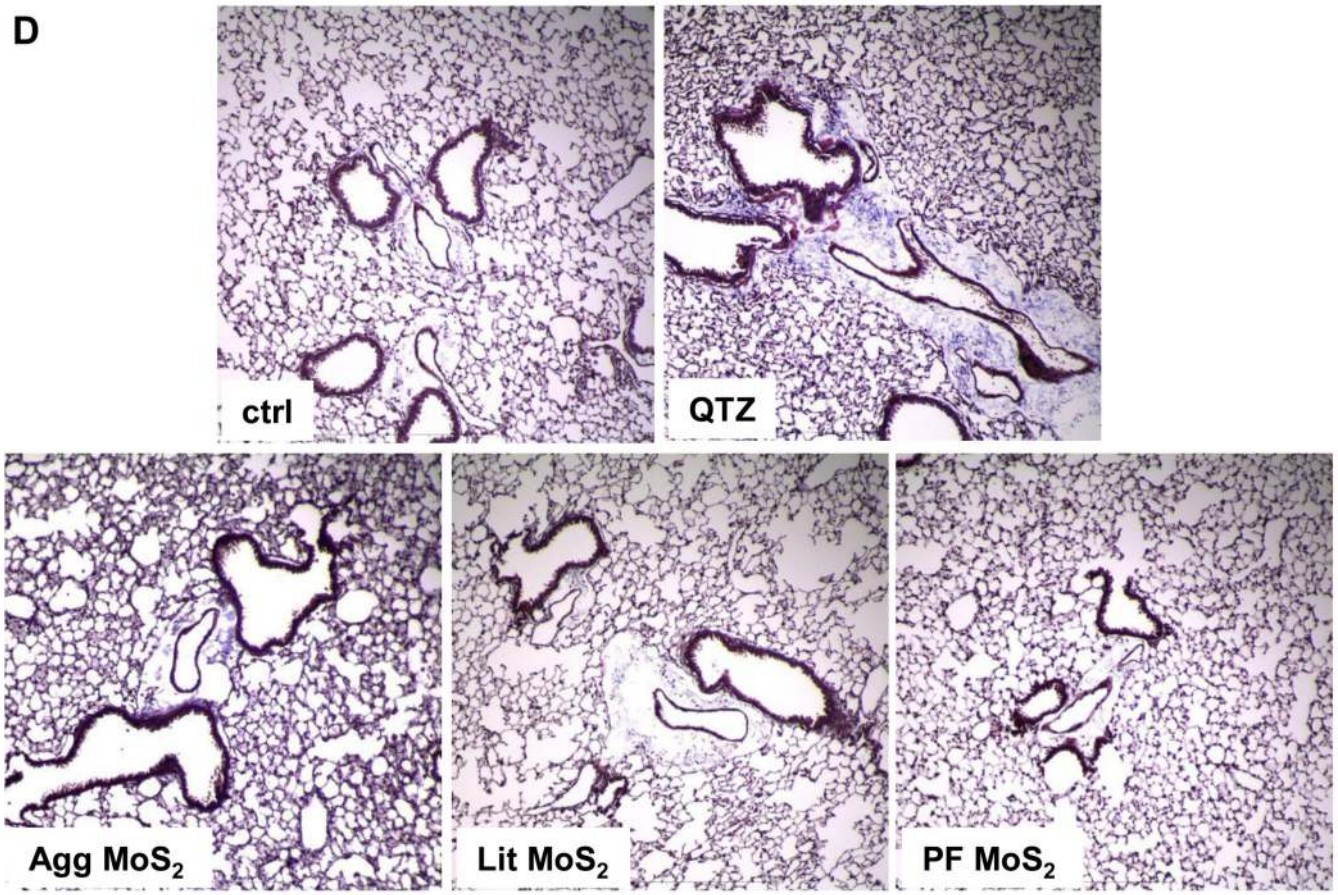

Figure 5.

Assessment of the possible fibrotic effects of MoS_2 materials 21 days after oropharyngeal installation. The experiment, described in Figure 4, was repeated with the exception that animal sacrifice was performed 21 days after oropharyngeal inspiration of a similar particle dose. There were 6 animals in each group. After the animals were euthanized, BALF was collected to determine TGF-β1 (A) and PDGF-AA (B) levels. (C) Total collagen content of the lung tissue was determined using the Sircol collagen kit (Biocolor Ltd., Carrickfergus, U.K.). *$p < 0.05$ compared with control. (D) Collagen deposition in the lung as determined by Masson's trichrome staining. Lung tissue was embedded, sectioned, stained with the Masson's trichrome and observed at 100 × magnification. Blue staining represents collagen deposition in the lung. Animals exposed to Quartz (QTZ) served as positive control.

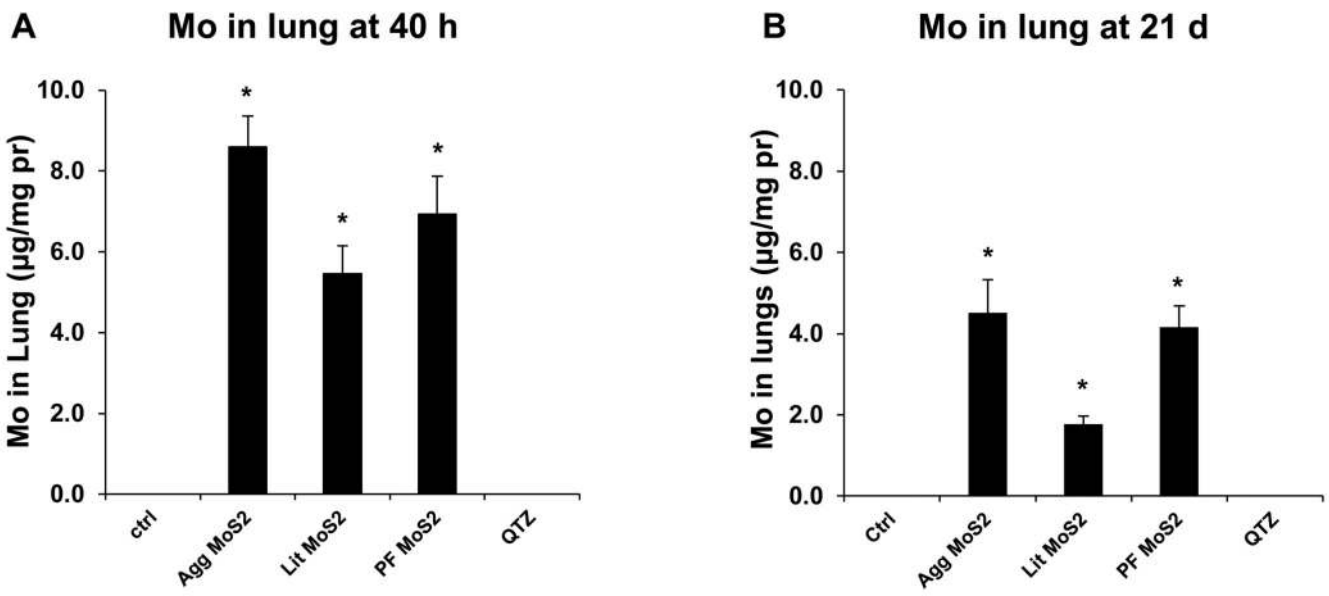

Figure 6.

Comparison of the Mo content in lung, 40 h (A) and 21 d (B) post-exposure as determined by ICP-OES. The lung tissues from the experiments in Figure 4 and 5 were collected and digested by concentrated nitric acid and hydrogen peroxide. The total Mo content in each lung sample was determined by ICP-OES.

Table 1
Characterization of MoS_2 materials in cell culture media

	In H_2O		In cRPMI1640		In BEGM	
	ζ [mV]	**d_H [nm]**	**ζ [mV]**	**d_H [nm]**	**ζ [mV]**	**d_H [nm]**
Agg-MoS_2	−23.6 ± 0.4	1334.8±47.8	−5.4±1.9	540.8±18.1	−8.8±1.6	1144.7±152.5
Lit-MoS_2	−34.3 ± 0.1	506.3±11.8	−7.7±3.0	585.6±17.3	−4.3±0.5	746.4±100.3
PF87-MoS_2	−12.9 ± 1.2	72±0.8	−7.8±1.3	80.1±0.8	−8.5±1.4	78.4±0.7

The zeta potential was measured using a ZetaSizer Nano-ZS (Malvern Instruments, Worcestershire WR, UK). The hydrodynamic diameters in H_2O, RPMI 1640 and BEGM were determined using high throughput dynamic light scattering (HT-DLS, Dynapro Plate Reader, Wyatt Technology).